C-12 *vs* C-3 substituted bile salts: An example of the effects of substituent position and orientation on the self-assembly of steroid surfactant isomers

Jacopo Cautela[a,3], Emilia Severoni[a,3], Carlos Redondo-Gómez[b,1,3], Maria Chiara di Gregorio[a,2], Alessandra Del Giudice[a], Simona Sennato[c,d], Roberta Angelini[c,d], Marco D'Abramo[a], Karin Schillén[e], Luciano Galantini[a,*]

[a] *Department of Chemistry, Sapienza University of Rome, P.le A. Moro 5, 00185 Rome, Italy*
[b] *Escuela de Química, Centro de Investigación en Electroquímica y Energía Química (CELEQ), Universidad de Costa Rica, San José, Costa Rica*
[c] *CNR-ISC Sede Sapienza, Sapienza University of Rome, P. le A. Moro 5, 00185 Roma, Italy*
[d] *Department of Physics, Sapienza University of Rome, P. le A. Moro 5, 00185 Roma, Italy*
[e] *Division of Physical Chemistry, Department of Chemistry, Lund University, P.O. Box 124, SE-221 00 Lund, Sweden*

ARTICLE INFO

ABSTRACT

Biomolecule derivatives are transversally used in nanotechnology. Deciphering their aggregation behavior is a crucial issue for the rational design of functional materials. To this end, it is necessary to build libraries of selectively functionalized analogues and infer general rules. In this work we enrich the highly applicative oriented collection of steroid derivatives, by reporting a rare example of C-12 selectively modified bile salt. While nature often exploits such position to encode functions, it is unusual and not trivial to prepare similar analogues in the laboratory. The introduction of a *tert*-butyl phenyl residue at C-12 provided a molecule with a self-assembly that remarkably switched from rigid pole-like structures to twisted ribbons at a biologically relevant critical temperature ($\sim 25\,°C$). The system was characterized by microscopy and spectroscopy techniques and compared with the C-3 functionalized analogue. The twisted ribbons generate samples with a gel texture and a viscoelastic response. The parallel analysis of the two systems suggested that the observed thermoresponsive self-assemblies occur at similar critical temperatures and are probably dictated by the nature of the substituent, but involve aggregates with different structures depending on position and orientation of the substituent. This study highlights the self-assembly properties of two appealing thermoresponsive systems. Moreover, it adds fundamental insights hereto missing in the investigations of the relation between self-assembly and structure of synthetic steroids, which are valuable for the rational design of steroidal amphiphiles.

1. Introduction

Nature provides a large set of molecules, called steroids, which are characterized by a common stiff molecular motif of four condensed rings that are found both in plant and animal species and that fulfill diverse and crucial biological functions such as signaling, membrane fluidity regulation, antibiotic and detergent activities [1–3]. The versatility of such compounds in natural processes promotes the steroid molecular motif as an appealing substrate for the construction of new molecules that expand the functions of the natural precursors and in turn allow the researchers to explore the potential of steroid derivatives

in a large set of application fields including biotechnology [4–6], catalysis [7,8], material science [9–14] and drug [15–18] and carrier [19,20] design. By following this approach, the steroid molecular backbone has been used in particular as a fundamental framework in the preparation of a set of rigid amphiphiles. For their synthesis, bile salts (BS) — a class of steroidal natural surfactants mainly acting as emulsifiers of dietary fats in mammals [21] — have been mainly used as precursors due to their intrinsic amphiphilicity and the presence of many functionalizable groups [22,23]. The modified molecules, usually identified as bile salt derivatives (BSDs), provide rigid building blocks for the fabrication of intriguing self-assembled nanostructures. These

---

rigid elements are indeed particularly prone to pack into ordered frameworks stabilized by hydrophobic interactions, hydrogen bonds and other geometrically constrained interactions depending on the substituents [24]. Natural amphiphiles like BSs provide important self-assembling molecules for the preparation of environmentally friendly and biocompatible materials that are also relevant for biomedical applications [25–27]. Chemical modifications on these molecules can be exploited to introduce additional functionalities and self-assembly features which can result in derivatives with improved performances.

Most BSs bear some OH groups on their steroid backbone at C-3, C-12 and C-7. Number, position and orientation (α or β) of these groups depend on the bile salt families. Specific modifications have provided so far self-assembling molecules with several appealing features. For instance, many derivatives associate into one directional aggregates, like fibrils and tubular structures. The cross section of the tubules spans a wide interval of diameters thus providing tools for applications at different scales. Remarkable derivatives have been synthesized by introducing amino acid [28–35] or sugar [36–38] substituents to provide molecules where features of peptides/saccharides and amphiphilic steroids are merged. Relevant systems are also those obtained by molecules bearing aromatic groups: they can aggregate into different elongated morphologies (e.g. tubules, fibers, ribbons) often through stimuli (pH, temperature, ionic strength) responsive self-assembly [39–43]. Interesting behaviors are also observed in mixtures of cationic/anionic analogues [44,45] or derivative/precursor [36], which are able to assemble into tubules with composition controlled charge and cross section, respectively. These features make BSD aggregates versatile tools for applications in different environments [22,35,46–49]. In particular, we observed recently that BSD tubules are suitable elements for higher order self-assembly, namely the supracolloidal aggregates [50]. This result highlights a novel employment of supramolecular tubules, opening up for the implementation of new functional materials.

Modification of BSs has been extensively investigated at the end of the lateral chain and at the C-3 by substituting the original OH [22,23]. However, a selective functionalization has been only seldom performed at the other OH bearing carbons C-7 and C-12, which are generally more hindered to substitution. It is interesting to remark that the steroid functionalization at C-12 is a particularly challenging issue that has involved both industry [51] and academic research, since many natural and synthetic C-12 substituted steroids exhibited pharmaceutical [51,52,61,53–60], biological [62–65], optical [66] and catalytic [67] properties. Moreover, the effect of a selective modification at C-12 on the self-assembly of BSDs is still unexplored.
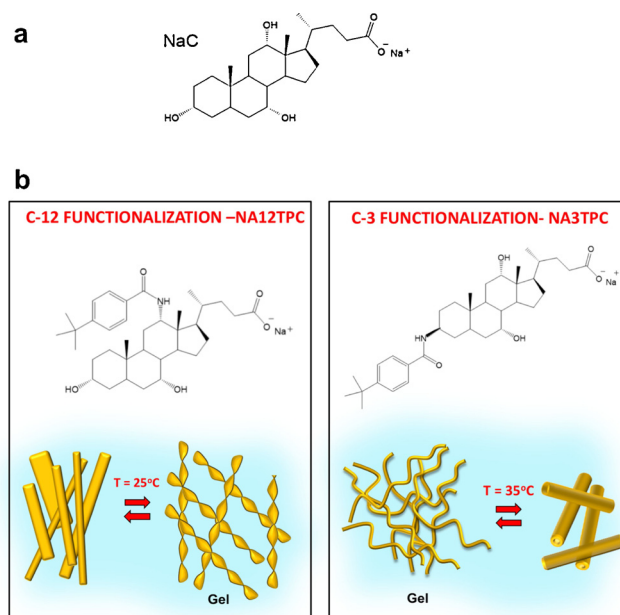
In this work we investigated the synthesis and the self-assembly behavior of a novel BSD (**Na12TPC**) obtained by selectively substituting the OH group at C-12α of sodium cholate (NaC) with a *p-tert*-butylphenylamide group (Scheme 1b, left).

The substituent was chosen in the light of the results previously obtained on the C-3β substituted analog (**Na3TPC** in Scheme 1b, right) that showed an astonishing thermoresponsive self-assembly into monodisperse tubular structures [41,42]. This knowledge allowed a comparison that represents a fundamental information to rationalize the effects of the substituted position on the BSDs self-assembly. The combination of different techniques such as dynamic light scattering (DLS), small angle X-ray scattering (SAXS), circular dichroism (CD), conventional and cryogenic transmission electron microscopy (TEM and Cryo-TEM), atomic force microscopy (AFM) and rheology was used to characterize the BSD self-assembly.

2. Materials and methods

2.1. Synthesis of *Na12TPC*

The derivative **Na12TPC** was synthesized by following the synthetic route depicted in Scheme 2. The methyl ester **2** of cholic acid, obtained

Scheme 1. Scheme of molecular structures and self-assembly behaviors of sodium cholate (NaC, a) functionalized at C-12α (Na12TPC, b left) and C-3β (Na3TPC, b right) with a *p-tert*-butylphenylamide group.

as reported in the literature [68], was used as starting material.

Methyl ester **2** was selectively diacetylated in positions C-3 and C-7 to afford a free hydroxyl group at C-12 position in derivative **3**. This secondary alcohol was oxidised with pyridinium dichromate (PDC) to the 12-keto derivative **4** with a quantitative yield. Condensation with hydroxylamine afforded the oxyme **5**. Subsequently compound **5** was stereoselectively converted to the 12-amino derivative **6** first by hydrogenating through the Adams Catalyst and then by reducing through Zn and acetic acid. The so obtained secondary amine on C-12 allowed for the condensation with *p*-(*t*-butyl)benzoil chloride to afford amide **7**. Finally, quantitative hydrolysis of the protecting groups at C-3, C-7 and C-24 and conversion to the sodium salt allowed to obtain the desired product **8**.

Details on the chemicals, synthetic procedure and characterization of the compounds are reported in the Supplementary Information.
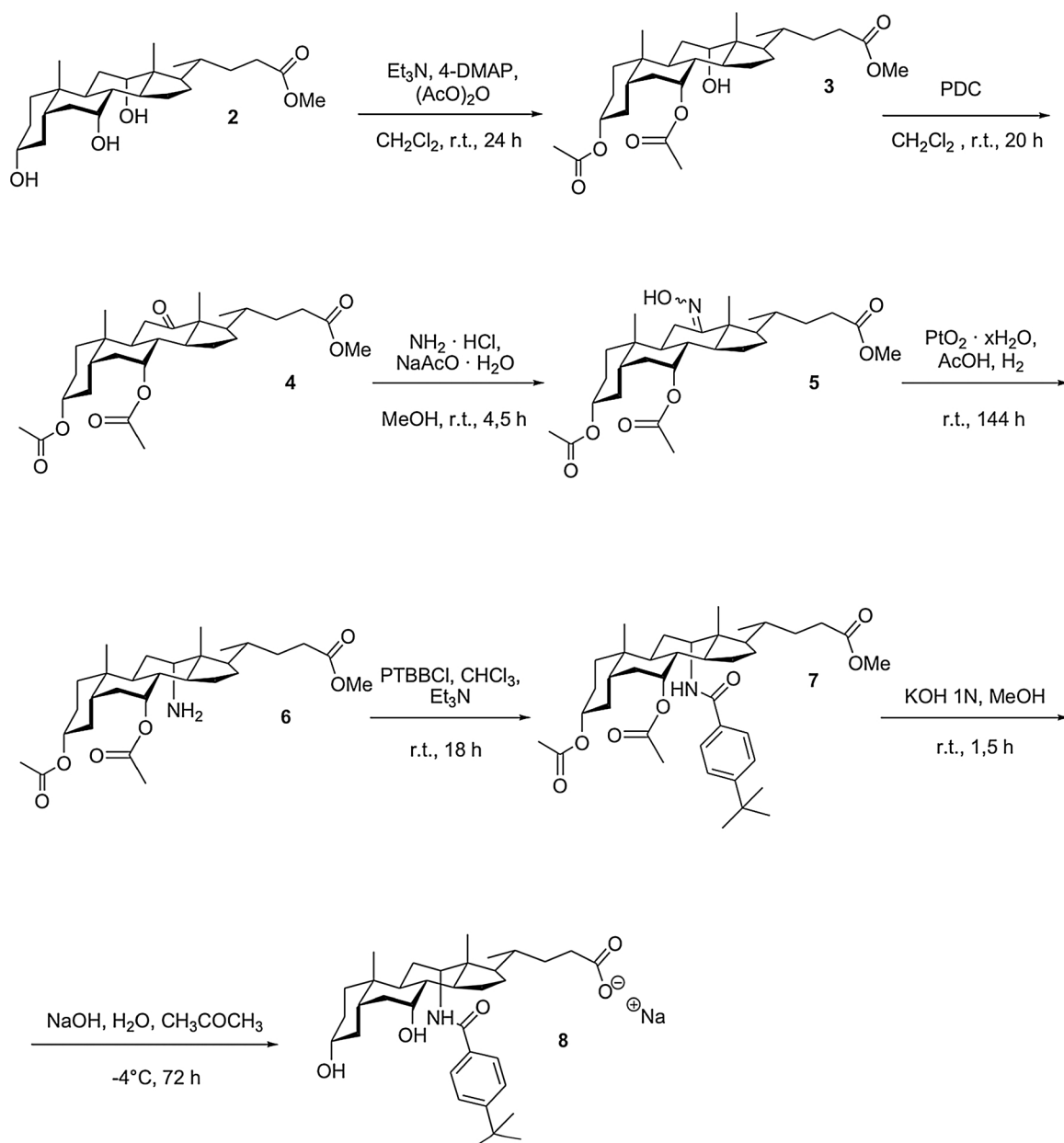
2.2. Sample preparation

The self-assembly of **Na12TPC** was investigated in alkaline conditions, obtained for all the samples by using sodium carbonate/bicarbonate buffer (pH 10.0) at total concentration ([Na$_2$CO$_3$] + [NaHCO$_3$]) of 6.0×10^{-2} M. The experiments were carried out on samples with a **Na12TPC** concentration of 1.0×10^{-2} M, unless otherwise stated. Measurement conditions and equipments are reported in the Supplementary Information.
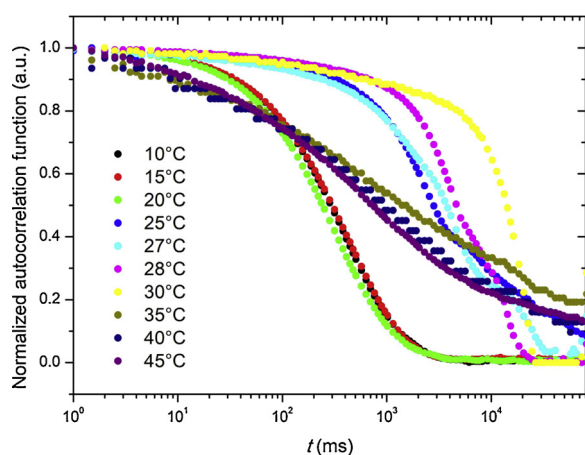
3. Results and discussion

3.1. *Na12TPC* self-assembly

Solubilization of **Na12TPC** did not occur at natural pH, as previously observed for the **Na3TPC** isomer as well as for many other BSDs. Based on the behavior reported for these molecules, high pH conditions (pH 10) were accomplished to guarantee deprotonation of the carboxylic group and facilitate solubilization, by using carbonate/bicarbonate buffer. Despite of this, the sample appeared as a turbid dispersion at 20 °C. However, different techniques highlighted thermoresponsive properties of such dispersion. The DLS intensity autocorrelation function showed an exponential decay at temperatures of

Scheme 2. Reaction sequence for the synthesis of Na12TPC.

Fig. 1. DLS normalized intensity autocorrelation function of Na12TPC 1.0×10^{-2} M in 6.0×10^{-2} M buffer, at different temperatures.

20 °C or lower. The intercept value of the autocorrelation function decreased and the curve flattened when the temperature was increased at 25–30 °C, indicating an arrest of the dynamics. The effect is reported in Fig. 1 where the curve were normalized to the same intercept.

UV spectra showed bands at 200 and 240 nm related to the π-π* transitions of the *tert*-butylphenylamide moiety (Fig. S1). In the same region CD signals were also observed. At room temperature the CD profile exhibited two oppositely signed bands around 240 (negative) and 220 (positive) and a positive intense signal at 190–200 nm. A temperature increase to 28 °C induced a consistent decrease in intensity at λ values < 230 nm (Fig. 2). Visually, a sol-gel transition in the sample was observed. By plotting the CD intensity at the representative wavelengths of 209 nm, as a function of temperature, a sigmoidal trend with inflection point at temperature around 25 °C was obtained (Fig. 2b). Such profile is typical of cooperatively responsive systems. The inferred inflection point falls in the same temperature range where the DLS experiments presented the slowing down of the dynamics in the system. Furthermore, the CD curves were similar to those recorded for
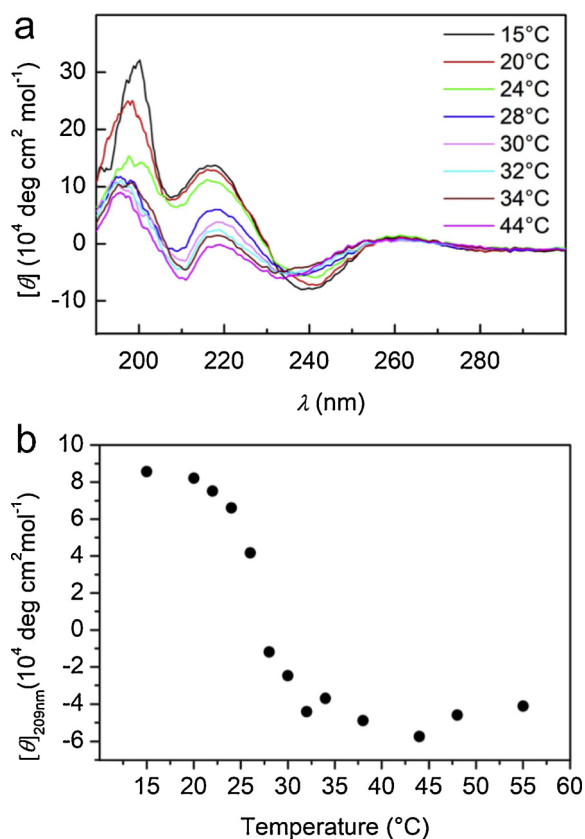
Fig. 2. CD spectra (a) of Na12TPC 1.0×10^{-2} M in 6.0×10^{-2} M buffer and molar ellipticity values at representative wavelength of 209 nm $[\theta]_{209nm}$, (b) of Na12TPC 1.0×10^{-2} M in 6.0×10^{-2} M buffer as a function of the temperature.

diluted (1.0×10^{-3} M) **Na12TPC** solution in ethanol and obtained by means of TD-DFT calculations (Fig. S2a). This suggests that the CD signal is mainly related to the chirality of the monomer and poorly affected by supramolecular interaction of the aromatic substituent in the aggregates forming in water. The calculated UV spectrum agreed rather well with the corresponding experimental one, with a major peak near 190 nm and a minor one near 230 nm (Figure S2b).

Cryo-TEM images showed that mainly pole-like structures with a polydisperse cross section were present in the sample at 20 °C (Fig. 3a,b), whereas twisted fibers were imaged at 35 °C both by Cryo-TEM (Fig. 3c–f) and AFM (Fig. S3). Such structures appeared straight and quite rigid. The fibers have a rectangular cross section with the wider side roughly 25 nm long and are twisted with a very regular pitch of about 80 ± 4 nm (Fig. 3e,f bottom, Fig. S4). Despite their remarkable length of tens of μm, the fibers do not crosslink. The low flexibility and the remarkable length hinder the rotation and other internal motions of the fibers, thus explaining the arrested dynamic inferred by DLS and the gel texture of the sample at the higher temperature. The regular shape of the "poles" suggests that they have and ordered arrangement of the constituting molecules. In addition, we observed that when the pole samples were aged for a few days under stirring at 20 °C, they did not show the same responsive behavior: the dispersions in this case must be heated close to the boiling point to be solubilized and subsequently cooled to obtain the gel of fibers. According with this behavior, we believe that the poles can turn into large stable crystals by aging. The formation of fibers in a sample initially containing the pole structures can be appreciated at a critical temperature value during the increasing temperature scan as the poles are small and in a metastable partially ordered or pre-crystalline state.

SAXS measurements confirmed the morphological properties of the fibers observed by microscopy. At $q < 0.2$ nm^{-1} the log-log plot follows the trend $I(q) \sim q^{-2}$ (Fig. 4), in agreement with previous reports on long twisted ribbons [69–72]. The IFT analysis of the $qI(q)$ vs q curve provided an asymmetric profile of the cross section pair distribution
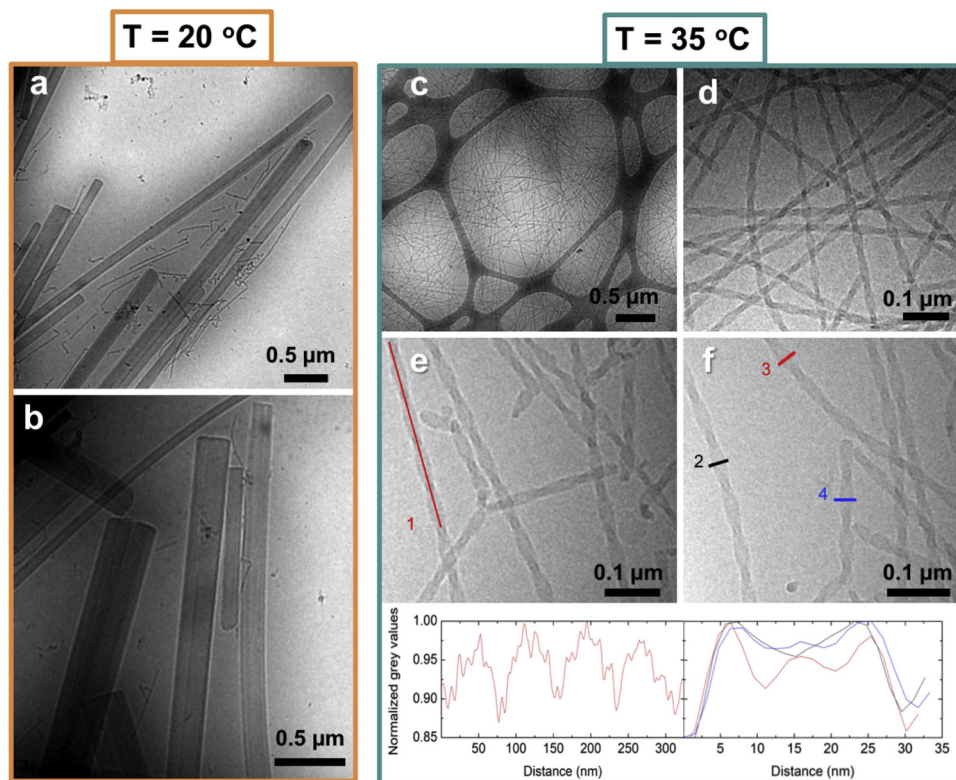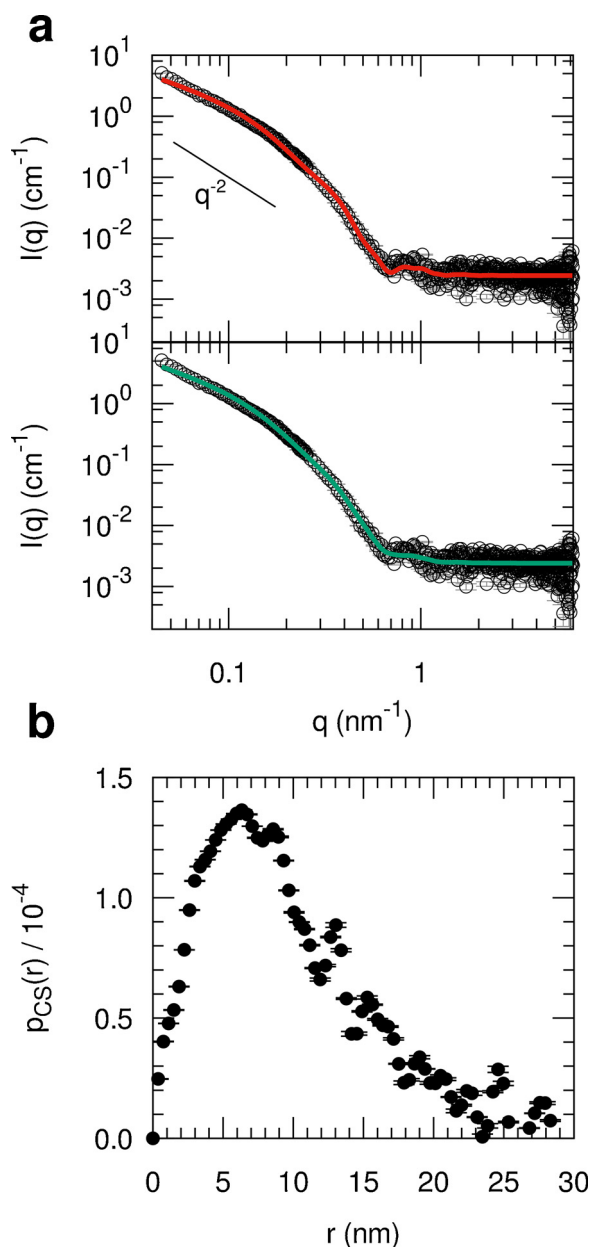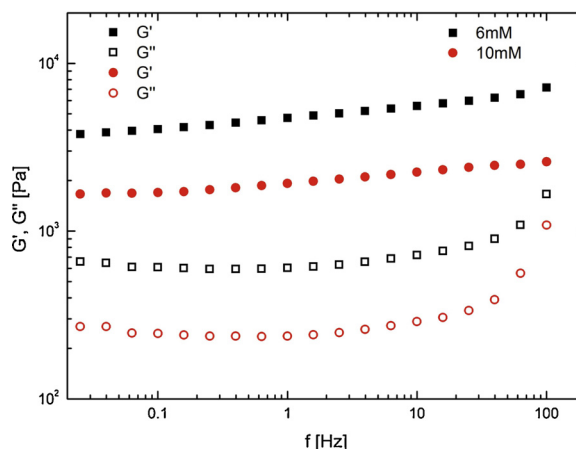

Fig. 3. Cryo-TEM micrographs of Na12TPC 1.0×10^{-2} M in 6.0×10^{-2} M buffer at 20 °C (a, b) and 35 °C (c–f). Intensity profile analysis of the structures labeled in e and f are reported below the relative panels.

Fig. 4. SAXS data of Na12TPC 1.0×10^{-2} M in 6.0×10^{-2} M buffer (a, empty circles) and relative fits by using the form factor of a long parallelepiped (a, top, red line) and the form factor of a long cylinder with elliptical cross-section (a, bottom, green line). Cross section pair distribution function $p_{cs}(r)$ (b).

Fig. 5. Elastic G′ (filled symbols) and viscous G″ (empty symbols) moduli as a function of frequency for gels of Na12TPC 6.0×10^{-3} M (black square) and Na12TPC 1.0×10^{-2} M (red circles) in 6.0×10^{-2} M buffer at 35 °C, strain amplitude $\gamma = 0.1$ %.
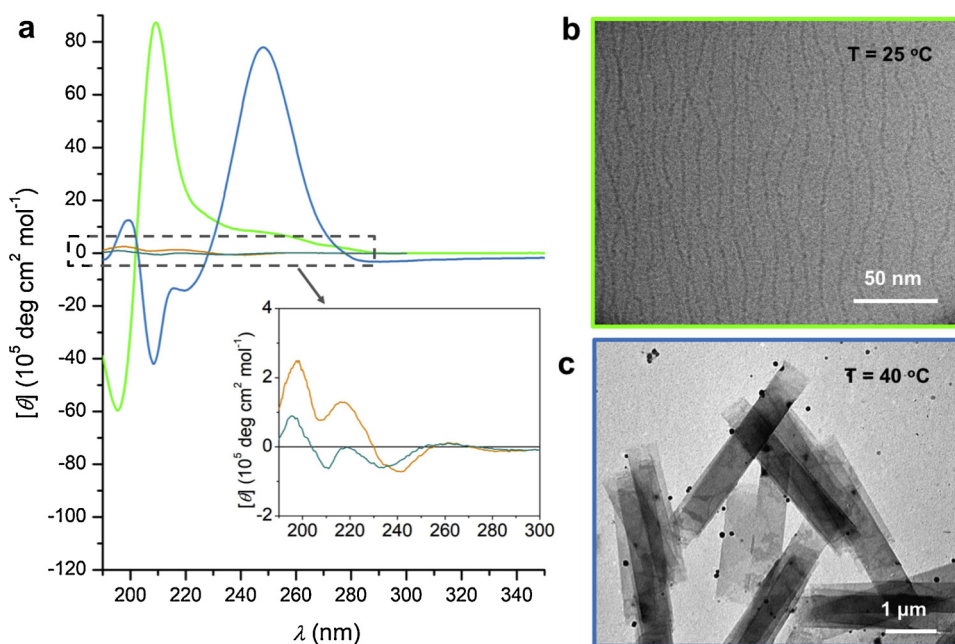
3.2. Na12TPC – Na3TPC self-assembly comparison

Twisted elongated structures are generally formed by helically arranged molecules. When the molecules contain chromophores, this kind of arrangements provides very intense CD spectra. This happens for example in the case of the derivative substituted at C-3β **Na3TPC** previously studied [41,42]. For this derivative the formation of a gel at room temperature is observed which gives a bisignate Cotton Effect around 220 nm. A transition into microtubes with a complex CD profile spreading the whole range of the UV absorbance is induced by heating at critical temperatures similar to those reported for **Na12TPC**. The CD intensity is much lower in the case of **Na12TPC** fibers suggesting that the chromophores interact weakly in these structures (Fig. 6)

However, like for **Na3TPC,** the self-assembly of **Na12TPC** is thermoresponsive. The temperature induced transition occurred at convenient critical values around 25 °C for **Na12TPC** and 35–40 °C for **Na3TPC**. Position and orientation of the substituent also affect structure and stability of the self-assembled aggregates at low temperature where metastable poles are formed by **Na12TPC**. The poles turn into stable crystals by aging thereby loosing responsiveness, whereas stable gel fibrils are provided by the C-3 substituted isomer.

4. Conclusions

A derivative of sodium cholate selectively substituted at C-12α by a *p-tert*-butylphenylamide group was analyzed in this work and compared with the C-3β substituted analogue. The results indicate that the substituent imparts similar features to the derivatives as both molecules exhibit a thermoresponsive self-assembly at high pH accomplished by carbonate/bicarbonate buffer. These outcomes of the two derivatives suggest some possible intrinsic features of the substituent. The different location and orientation of the substituent is reflected in very different aggregate structures. Metastable poles are formed by the C-12 substituted analogue at low temperature instead of the more stable gel fibrils provided by the isomer functionalized at C-3. Stiff twisted parallelepiped aggregates are given by the former instead of microtubes provided by the latter, upon heating the sample above critical temperatures around 25 and 35–40 °C, respectively. This study represents a first step in the construction of a library highlighting the effect of position and orientation of substituents on the self-assembly of bile salt derivative isomers, which is expected to be fundamental for a rational design of steroid based molecules for application.

function $p_{cs}(r)$ with maximum dimension around 28 nm (Fig. 4b), which suggests a rectangular shape of the fiber cross section. The experimental scattering profile could be fitted by using the form factor of a long parallelepiped with 9.4 nm x 27.9 nm cross section (Fig. 4), or alternatively the form factor of a long cylinder with elliptical cross-section having minor and major axes of 10.1 nm and 32.9 nm, respectively (details of the fits are reported in Table S1).

Dynamic rheology was used to investigate the mechanical features of the gel. Oscillatory experiments in strain sweep mode were first performed on the fibrillar hydrogel (6.0×10^{-3} M **Na12TPC**) at a fixed frequency of 1.0 Hz. Subsequently frequency sweep measurements were collected at a constant applied strain amplitude falling in the linear viscoelastic domain ($\gamma = 0.1$ %) to provide the frequency dependence of G′ and G″ (Fig. 5). G′ was found to be larger than G″ at all frequencies, as expected for a soft elastic solid.

Fig. 6. CD curves of Na3TPC 1.0×10^{-3} M in 3.0×10^{-2} M carbonate/bicarbonate buffer solution at 20 (a, light green line) and 40 °C (a, blue line) and of Na12TPC 1.0×10^{-2} M in 6.0×10^{-2} M buffer at 20 (a, orange line) and 40 °C (a, green line). Zoom in of the Na12TPC spectra are reported as inset in a. Cryo-TEM (b) and TEM (c) micrographs of Na3TPC 1.0×10^{-3} M in 3.0×10^{-2} M carbonate/bicarbonate buffer solution at 25 (b) and 40 °C (c).

Acknowledgments

Appendix A. Supplementary data

Supplementary material related to this article can be found, in the online version, at doi:https://doi.org/10.1016/j.colsurfb.2019.110556.

References

[1] R.A. Hill, H.L.J. Makin, D.N. Kirk, G.M. Murphy, Dictionary of Steroids, Taylor & Francis, 1991.

[2] C.A. Russell, G.K. Roberts, Chemical history: reviews of the recent literature, Chemistry, Cambridge, 2005 in: T. R. S. (Ed.).

[3] G.P. Moss, Nomenclature of steroids. Recommendations 1989, Eur. J. Biochem. 186 (1989) 429–458.

[4] L. Fernández-Cabezón, B. Galán, J.L. García, New insights on steroid biotechnology, Front. Microbiol. 9 (2018) 958.

[5] J. Mckenna, J.M. McKenna, D.W. Thornthwaite, Bis-steroids as potential enzyme models: perylene solubilisation and dye spectral changes with aqueous solutions of some derivatives of conessine and cholic acid, J. Chem. Soc. Chem. Commun. 0 (1977) 809.

[6] A. Sochanik, I. Kaida, I. Mitrus, A. Rajca, S. Szala, A new cholesterol derivative suitable for transfecting certain type of cells in the presence of 10% serum, Cancer Gene Ther. 7 (2000) 513–520.

[7] D.B. Ramachary, R. Sakthidevi, P.S. Reddy, Direct organocatalytic stereoselective transfer hydrogenation of conjugated olefins of steroids, RSC Adv. 3 (2013) 13497–13506.

[8] S.D. Fried, S. Bagchi, S.G. Boxer, Extreme electric fields power catalysis in the active site of ketosteroid isomerase, Science 346 (2001) 1510–1514.

[9] R. Lettieri, D. Monti, K. Zelenka, T. Trnka, P. Drašar, M. Venanzi, Glucosylated steroid-porphyrins as new tools for nanotechnology applications, New J. Chem. 36 (2012) 1246–1254.

[10] Y.-G. Jia, C. Malveau, M.A. Mezour, D.F. Perepichka, X.X. Zhu, Molecular necklace: threadingb-cyclodextrins onto polymers derived from bile acids, Angew. Chem. Int. Ed. 128 (2016) 12158–12162.

[11] R. Natarajan, L. Bridgland, A. Sirikulkajorn, J.H. Lee, M.F. Haddow, G. Magro, B. Ali, S. Narayanan, P. Strickland, J.P.H. Charmant, et al., Tunable porous organic crystals: structural scope and adsorption properties of nanoporous steroidal ureas, J. Am. Chem. Soc. 135 (2013) 16912–16925.

[12] F. Le Bideau, S. Dagorne, Synthesis of transition-metal steroid derivatives, Chem. Rev. 113 (2013) 7793–7850.

[13] A.L. Sisson, V. Del Amo Sanchez, G. Magro, A.M.E. Griffin, S. Shah, J.P.H. Charmant, A.P. Davis, Spiraling steroids: organic crystals with asymmetric nanometer-scale channels, Angew. Chem. Int. Ed. 44 (2005) 6878–6881.

[14] X.X. Zhu, M. Nichifor, Polymeric materials containing bile acids, Acc. Chem. Res. 35 (2002) 539–546.

[15] L. Nahar, S.D. Sarker, Steroid Dimers: Chemistry and Applications in Drug Design and Delivery, John Wiley & Sons, 2012.

[16] N.A. Evans, Current concepts in anabolic-androgenic steroids, Am. J. Sports Med. 32 (2004) 534–542.

[17] V.A. D'yakonov, R.A. Tuktarova, L.U. Dzhemileva, S.R. Ishmukhametova, M.M. Yunusbaeva, U.M. Dzhemilev, Catalytic cyclometallation in steroid chemistry V: synthesis of hybrid molecules based on steroid oximes and (5Z,9Z)-Tetradeca-5,9-Dienedioic acid as potential anticancer agents, Steroids 138 (2018) 14–20.

[18] W.S. Kim, K. Du, A. Eastman, R.P. Hughes, G.C. Micalizio, Synthetic nat-or ent-steroids in as few as five chemical steps from Epichlorohydrin, Nat. Chem. 10 (2018) 70–77.

[19] H. Valkenier, A.P. Davis, Making a match for valinomycin: steroidal scaffolds in the design of electroneutral, electrogenic anion carriers, Acc. Chem. Res. 46 (2013) 2898–2909.

[20] P.R. Brotherhood, A.P. Davis, Steroid-based anion receptors and transporters, Chem. Soc. Rev. 39 (2010) 3633.

[21] D. Madenci, S.U. Egelhaaf, Self-assembly in aqueous bile salt solutions, Curr. Opin. Colloid Interface Sci. 15 (2010) 109–115.

[22] M.C. di Gregorio, L. Travaglini, A. Del Giudice, J. Cautela, N.V. Pavel, L. Galantini, Bile salts: natural surfactants and precursors of a broad family of complex amphiphiles, Langmuir 35 (2019) 6803–6821.

[23] L. Galantini, M.C. di Gregorio, M. Gubitosi, L. Travaglini, J. Vázquez, A. Jover, F. Meijide, V.H. Soto, N.V. Pavel, Bile salts and derivatives : rigid unconventional amphiphiles as dispersants, carriers and superstructure building blocks, Curr. Opin. Colloid Interface Sci. 20 (2015) 170–182.

[24] P. Terech, S. Dourdain, S. Bhat, U. Maitra, Self-assembly of bile steroid analogues: molecules, fibers, and networks, J. Phys. Chem. B 113 (2009) 8252–8267.

[25] C. Faustino, C. Serafim, P. Rijo, C.P. Reis, Bile acids and bile acid derivatives: use in drug delivery systems and as therapeutic agents, Expert Opin. Drug Deliv. 13 (2016) 1133–1148.

[26] A.J. Cunningham, M. Robinson, X. Banquy, J. Leblond, X.X. Zhu, Bile acid-based drug delivery systems for enhanced doxorubicin encapsulation: comparing hydrophobic and ionic interactions in drug loading and release, Mol. Pharm. 15 (2018) 1266–1276.

[27] E. Tasca, A. Del Giudice, L. Galantini, K. Schillén, A.M. Giuliani, M. Giustini, A fluorescence study of the loading and time stability of doxorubicin in sodium cholate/PEO-PPO-PEO triblock copolymer mixed micelles, J. Colloid Interface Sci. 540 (2019) 593–601.

[28] L. Travaglini, M. Gubitosi, M.C. di Gregorio, N.V. Pavel, A. D'Annibale, M. Giustini, V.H. Soto Tellini, J. Vázquez Tato, M. Obiols-Rabasa, S. Bayati, L. Galantini, On the self-assembly of a tryptophan labeled deoxycholic acid, Phys. Chem. Chem. Phys. 16 (2014) 19492–19504.

[29] L. Travaglini, M. Gubitosi, M.C. di Gregorio, A. D'Annibale, F. Meijide, M. Giustini, S. Sennato, M. Obiols-Rabasa, K. Schillén, N.V. Pavel, et al., A tryptophan-substituted cholic acid: expanding the family of labelled biomolecules, Colloids Surf. A 483 (2015) 142–149.

[30] L. Travaglini, A. D'Annibale, K. Schillén, U. Olsson, S. Sennato, N.V. Pavel, L. Galantini, Amino acid–bile acid based molecules: extremely narrow surfactant nanotubes formed by a phenylalanine-substituted cholic acid, Chem. Commun. 48 (2012) 12011–12013.

[31] L. Travaglini, C. Giordano, A. D'Annibale, M. Gubitosi, M.C. di Gregorio, K. Schillén, A. Stefanucci, A. Mollica, N.V. Pavel, L. Galantini, Twisted nanoribbons from a RGD-bearing cholic acid derivative, Colloids Surf. B 159 (2017) 183–190.

[32] L. Travaglini, A. D'Annibale, M.C. di Gregorio, K. Schillén, U. Olsson, S. Sennato, N.V. Pavel, L. Galantini, Between peptides and bile acids: self-assembly of phenylalanine substituted cholic acids, J. Phys. Chem. B 117 (2013) 9248–9257.

[33] L. Travaglini, M.C. di Gregorio, E. Severoni, A.D. Annibale, S. Sennato, F. Tardani, M. Giustini, M. Gubitosi, A. Del, L. Galantini, Deoxycholic acid and l -Phenylalanine enrich their hydrogel properties when combined in a zwitterionic derivative, J. Colloid Interface Sci. 554 (2019) 453–462.

[34] M. Maity, U. Maitra, Supramolecular gels from conjugates of bile acids and amino acids and their applications, Eur. J. Org. Chem. 2017 (2017) 1713–1720.

[35] V. Noponen, A. Valkonen, M. Lahtinen, H. Salo, E. Sievänen, Self-assembly properties of bile acid derivatives of L-cysteine, L-valine and L-serine alkyl esters, Supramol. Chem. 25 (2013) 133–145.

[36] M. Gubitosi, L. Travaglini, M.C. di Gregorio, N.V. Pavel, J. Vazquez-Tato, S. Sennato, U. Olsson, K. Schillén, L. Galantini, Tailoring supramolecular nanotubes by bile salt based surfactant mixtures, Angew. Chem. Int. Ed. 54 (2015) 7018–7021.

[37] M. Gubitosi, L. Travaglini, A. D'Annibale, N.V. Pavel, J. Vázquez Tato, M. Obiols-Rabasa, S. Sennato, U. Olsson, K. Schillén, L. Galantini, Sugar-bile acid-based bolaamphiphiles: from scrolls to monodisperse single-walled tubules, Langmuir 30 (2014) 6358–6366.

[38] M. Gubitosi, F. Meijide, A. D'Annibale, J. Vázquez Tato, A. Jover, L. Galantini, L. Travaglini, M.C. di Gregorio, N.V. Pavel, Crystal structure of a Lithium salt of a glucosyl derivative of lithocholic acid, Steroids 113 (2016) 87–94.

[39] M.C. di Gregorio, N.V. Pavel, A. Jover, F. Meijide, J. Vázquez Tato, V.H. Soto Tellini, A.A. Vargas, O. Regev, Y. Kasavi, K. Schillén, et al., PH sensitive tubules of a bile acid derivative: a tubule opening by release of wall leaves, Phys. Chem. Chem. Phys. 15 (2013) 7560–7566.

[40] M.C. di Gregorio, M. Varenik, M. Gubitosi, L. Travaglini, N.V. Pavel, A. Jover, F. Meijide, O. Regev, L. Galantini, Multi stimuli response of a single surfactant presenting a rich self-assembly behavior, RSC Adv. 5 (2015) 37800–37806.

[41] L. Galantini, C. Leggio, A. Jover, F. Meijide, N.V. Pavel, V.H. Soto Tellini, J. Vázquez Tato, R. Di Leonardo, G. Ruocco, Kinetics of formation of supramolecular tubules of a sodium cholate derivative, Soft Matter 5 (2009) 3018–3025.

[42] M.C. di Gregorio, M. Gubitosi, L. Travaglini, N.V. Pavel, A. Jover, F. Meijide, J. Vázquez Tato, S. Sennato, K. Schillén, F. Tranchini, et al., Supramolecular assembly of a thermoresponsive steroidal surfactant with an oppositely charged thermoresponsive block copolymer, Phys. Chem. Chem. Phys. 19 (2017) 1504–1515.

[43] J.V. Trillo, F. Meijide, A. Jover, V.H. Soto, S. De Frutos, M.C. di Gregorio, L. Galantini, J. Vazquez-Tato, Self-aggregation mechanism of a naphthylamide cationic derivative of cholic acid. From fibers to tubules, RSC Adv. 4 (2014) 5598–5606.

[44] N. Manghisi, C. Leggio, A. Jover, F. Meijide, N.V. Pavel, V.H.S. Tellini, J.V. Tato, R.G. Agostino, L. Galantini, Catanionic tubules with tunable charge, Angew. Chem. Int. Ed. 49 (2010) 6604–6607.

[45] M.C. di Gregorio, E. Severoni, L. Travaglini, M. Gubitosi, S. Sennato, F. Mura, C. Redondo-Gomez, A. Jover, N.V. Pavel, L. Galantini, Bile acid derivative-based catanionic mixtures: versatile tools for superficial charge modulation of supramolecular lamellae and nanotubes, Phys. Chem. Chem. Phys. 20 (2018) 18957–18968.

[46] M. Gubitosi, J.V. Trillo, A. Alfaro Vargas, N.V. Pavel, D. Gazzoli, S. Sennato, A. Jover, F. Meijide, L. Galantini, Characterization of carbon nanotube dispersions in solutions of bile salts and derivatives containing aromatic substituents, J. Phys. Chem. B 118 (2014) 1012–1021.

[47] K. Margulis-Goshen, M.C. di Gregorio, N.V. Pavel, L. Abezgauz, D. Danino, J. Vázquez Tato, V.H. Soto Tellini, S. Magdassi, L. Galantini, Drug-loaded nanoparticles and supramolecular nanotubes formed from a volatile microemulsion with

[48] A. Chakrabarty, U. Maitra, Organogels from dimeric bile acid esters: in situ formation of gold nanoparticles, J. Phys. Chem. B 117 (26) (2013) 8039–8046.

[49] J. Rohacova, M.L. Marín, A. Martinez-Romero, L. Diaz, J.E. O'Connor, M.J. Gomez-Lechon, M.T. Donato, J.V. Castell, M.A. Miranda, Fluorescent benzofurazan-cholic acid conjugates for in vitro assessment of bile acid uptake and its modulation by drugs, ChemMedChem 4 (2009) 466–472.

[50] J. Cautela, V. Lattanzi, L. Månsson, L. Galantini, J.J. Crassous, Sphere–Tubule superstructures through supramolecular and supracolloidal assembly pathways, Small 14 (2018) 1803215.

[51] Y.Y. See, A.T. Herrmann, Y. Aihara, P.S. Baran, Scalable C-H oxidation with copper: synthesis of polyoxypregnanes, J. Am. Chem. Soc. 137 (2015) 13776–13779.

[52] V. Gupta, A. Kumar, A. Khare, N.K. Khare, Pregnane and pregnane tetraglycoside from Marsdenia roylei, Nat. Prod. Res. 25 (2011) 959–973.

[53] J. Kolodziejczyk-Czepas, A. Stochmal, Bufadienolides of Kalanchoe species: an overview of chemical structure, biological activity and prospects for pharmacological use, Phytochem. Rev. 16 (2017) 1155–1171.

[54] D. Li, J.I. Williams, R.J. Pietras, Squalamine and cisplatin block angiogenesis and growth of human ovarian Cancer cells with or without HER-2 gene overexpression, Oncogene 21 (2002) 2805–2814.

[55] M.A. Rahman, M. Bam, E. Luat, M.S. Jui, M.S. Ganewatta, T. Shokfai, M. Nagarkatti, A.W. Decho, C. Tang, Macromolecular-clustered facial amphiphilic antimicrobials, Nat. Commun. 9 (2018) 1–10.

[56] B. Ding, Q. Guan, J.P. Walsh, J.S. Boswell, T.W. Winter, E.S. Winter, S.S. Boyd, C. Li, P.B. Savage, Correlation of the antibacterial activities of cationic peptide antibiotics and cationic steroid antibiotics, J. Med. Chem. 45 (2002) 663–669.

[57] P. Geoffroy, B. Ressault, E. Marchioni, M. Miesch, Synthesis of hoodigogenin a, aglycone of natural appetite suppressant glycosteroids extracted from Hoodia gordonii, Steroids 76 (2011) 702–708.

[58] J. Zhang, H. Shi, Y. Ma, B. Yu, Expeditious synthesis of saponin P57, an appetite suppressant from Hoodia plants, Chem. Commun. 48 (2012) 8679–8681.

[59] K.C. Fortner, D. Kato, Y. Tanaka, M.D. Shair, Enantioselective Synthesis of (+) -Cephalostatin 1, (2010), pp. 275–280.

[60] S.-Q. Luo, L.-Z. Lin, G.A. Cordell, L. Xue, M.E. Johnson, Polyoxypregnanes from Marsdenia tenacissima, Phytochemistry 34 (1993) 1615–1620.

[61] P.B. Savage, C. Li, U. Taotafa, B. Ding, Q. Guan, Antibacterial properties of cationic steroid antibiotics, FEMS Microbiol. Lett. 217 (2002) 1–7.

[62] H. Li, H. Valkenier, L.W. Judd, P.R. Brotherhood, S. Hussain, J.A. Cooper, O. Jurček, H.A. Sparkes, D.N. Sheppard, A.P. Davis, Efficient, non-toxic anion transport by synthetic carriers in cells and epithelia, Nat. Chem. 8 (2016) 24–32.

[63] X. Wu, L.W. Judd, E.N.W. Howe, A.M. Withecombe, V. Soto-Cerrato, H. Li, N. Busschaert, H. Valkenier, R. Pérez-Tomás, D.N. Sheppard, et al., Nonprotonophoric electrogenic Cl− transport mediated by valinomycin-like carriers, Chem 1 (2016) 127–146.

[64] H.P. Hsieh, J.G. Muller, C.J. Burrows, Synthesis and DNA binding properties of C3-, C12-, and C24- substituted amino-steroids derived from bile acids, Bioorg. Med. Chem. 3 (1995) 823–838.

[65] R. Edenharder, Dehydroxylation of cholic acid at C12 and epimerization at C5 and C7 by Bacteroides species, J. Steroid Biochem. 21 (1984) 413–420.

[66] M. Gomez-Mendoza, M.L. Marin, M.A. Miranda, Photoactive bile salts with critical micellar concentration in the micromolar range, Phys. Chem. Chem. Phys. 18 (2016) 12976–12982.

[67] G.L. Puleo, M. Masi, A. Iuliano, Synthesis of proline derivatives of bile acids and their evaluation as organocatalysts in the asymmetric direct aldol reaction, Tetrahedron Asymmetry 18 (2007) 1364–1375.

[68] S. Gouin, J.X.X. Zhu, Synthesis of 3α- and 3β-dimers from selected bile acids, Steroids 61 (1996) 664–669.

[69] I.W. Hamley, Form factor of helical ribbons, Macromolecules 41 (2008) 8948–8950.

[70] H. Cui, T. Muraoka, A.G. Cheetham, S.I. Stupp, Self-assembly of giant peptide nanobelts, Nano Lett. 9 (2009) 945–951.

[71] J.E. Goldberger, E.J. Berns, R. Bitton, C.J. Newcomb, S.I. Stupp, Electrostatic control of bioactivity, Angew. Chem. Int. Ed. 50 (2011) 6292–6295.

[72] A.S. Cuvier, J. Berton, C.V. Stevens, G.C. Fadda, F. Babonneau, I.N.A. Van Bogaert, W. Soetaert, G. Pehau-Arnaudet, N. Baccile, PH-triggered formation of nanoribbons from yeast-derived glycolipid biosurfactants, Soft Matter 10 (2014) 3950–3959.